In situ Diagnostics in Plasmas of Electronic-Ground-State Hydrogen Molecules in High Vibrational and Rotational States by Laser-Induced Fluorescence with Vacuum-Ultraviolet Radiation

Thomas Mosbach, H.-M. Katsch, and H. F. Döbele

Institut für Laser- und Plasmaphysik, Universität GH Essen, 45117 Essen, Germany

(Received 24 September 1999; revised manuscript received 27 July 2000)

Detection of excited electronic-ground-state hydrogen molecules with v'' up to 13 in a magnetic multipole plasma source was performed for the first time by laser-induced fluorescence with vacuum-ultraviolet radiation. The measurements are taken after fast shutoff of the discharge current. The rovibrationally excited molecules live longer than the plasma background light so that the fluorescence light can be detected with good signal-to-noise ratio. Absolute level populations are measured as well as decay times. The theoretically predicted suprathermal population of the vibrational distribution is clearly identified. The H^- density is calculated on the basis of the measured populations and the measured electron energy distribution function. It is in excellent agreement with the H^- density measured by photodetachment.

PACS numbers: 52.70.Kz, 52.20.–j

It is well known that molecular reaction rates in low temperature plasmas are critically dependent on vibrational and rotational excitation. Model calculations of plasma discharges have been developed which treat both the plasma state and the relevant rovibronic populations in a self-consistent manner. H_2 plays a prominent role in this context. It is the most simple molecular system, and its database is comparatively well developed. The experimental comparison of populations of highly excited vibrational and rotational states in hydrogen is, therefore, of particular importance, since it provides a sensitive test, better than with any other molecule, for the degree of our theoretical understanding of the population dynamics of molecular states in plasmas. The predictions of model calculations of high rovibronic state populations have found particular interest in connection with H^- densities in plasma sources, where these states are considered to play a key role in the production of H^- ions in volume processes. Negative hydrogen ions extracted from plasma sources are being applied to generate charged and neutral particle beams for accelerator systems. H^- ions in the MeV energy range are being considered as primary charged particles for neutral beam heating of fusion devices [1,2]. Magnetic multipole plasma sources have been found to have a surprisingly high content of H^- ions [3,4], and magnetic field configurations have been developed for optimization and efficient extraction [1,2,5]. There has been, however, a discussion extending over years on the underlying generation mechanisms of H^- ions and the factors determining the population [6–14]. Dissociative attachment of low energy electrons ($E \sim 1$ eV) to highly excited electronic-ground-state molecules is being considered as one of the most likely generation mechanisms:

$$e + H_2(X^1\Sigma_g^+(v'', J'')) \rightarrow H_2^-(^2\Sigma_{g/u}^+) \rightarrow H^- + H. \quad (1)$$

The cross section for this process increases by 5 orders of magnitude from $v'' = 0$ to $v'' = 5$, where it reaches a value about $\sim 10^{-16}$ cm^2. After a maximum at $v'' = 8$ (at a value about 10^{-15} cm^2) it reduces slightly [15–17]. An alternative channel for the formation of H^- is dissociative attachment of electrons to electronically excited states of H_2. High-lying Rydberg states have been discussed recently because of the large value of the attachment rate coefficient [13,14,18].

Numerical calculations of the population include a multitude of processes. Some of the cross sections involved can be considered as well established, whereas others are only known by order of magnitude. A survey is given in [19]. Simulations predict a suprathermal population of the high vibrational states. The main process of excitation into these states is the so-called "*E-V*" process [3,4,6,20] by electrons of energies in excess of 10 eV, i.e.,

$$e + H_2(X^1\Sigma_g^+(v_i'')) \rightarrow H_2^*(B^1\Sigma_g^+, C^1\Pi_u, \ldots, v'') + e \rightarrow H_2(X^1\Sigma_g^+(v_f'')) + e + h\nu. \quad (2)$$

An experimental verification of the results of the models is still lacking since suitable diagnostic techniques to determine populations of highly excited states of H_2 (and D_2) molecules in their electronic ground state were not available so far. Emission spectroscopy does not yield information, because these homonuclear electronic-ground-state molecules do not radiate. Attempts to diagnose vibrational state populations by coherent anti-Stokes Raman spectroscopy yielded results up to $v'' = 3$ [21], but were unable to contribute to the question on the population of higher states due to lack of sensitivity. Subsequent experiments with *ex situ* multiphoton ionization were able to obtain data up to $v'' = 5$ and found arguments in favor of the theoretically expected suprathermal population [22]. The vacuum-ultraviolet (VUV) absorption measurements at Lawrence Berkeley Laboratory [23,24] and by our group [25] represent a direct and quantitative approach but are still not sensitive enough to reach the relevant domain of v'' values (see Fig. 6 below). We have attempted the application of fluorescence diagnostics in the VUV for two

 0031-9007/00/85(16)/3420(4)$15.00

reasons: First, the metastable character of the states to be probed provides a simple means to overcome the plasma background light problem by fast interruption of the discharge current, and, second, our method of generation of VUV radiation — stimulated anti-Stokes Raman scattering in molecular hydrogen — allows us to excite a variety of suitable transitions.

The magnetic multipole plasma source has two tungsten filaments as cathodes; the body of the chamber is the anode. Magnets positioned on the outer surface of the chamber provide efficient confinement of the electrons. The source can be operated in the pulsed mode with the option to control "on" and "off" intervals independently. For the experiments reported here, the current of 0.5 A, the voltage is 100 V and the H_2 filling pressure is 1.5 Pa; the on interval lasts for $\sim$2 ms. For these parameters, the plasma radiation disappears typically within microseconds after current shutoff.

The spatial structure of the plasma is investigated by a Langmuir probe system. Figure 1 shows the electron energy distribution function (EEDF) for a plane between the filaments. The central section which is essentially field-free has a diameter of $\sim$6 cm. The central part is the section where the highly excited molecules are predominantly formed by the E-V process. Fast electrons with energies in excess of 20 eV could not be identified in our discharge.

The laser system consists of an excimer laser-pumped dye laser with pulse energies of 30–60 mJ in the spectral range 410–500 nm, pulse duration 15 ns, and bandwidth $\sim$0.2 cm^{-1}. With second-harmonic generation (SHG) in a BBO crystal, we have 4–8 mJ available for Raman shifting. The essentials of the Raman cell are described in [26]. With this scheme of VUV generation, all Raman orders (together with the depleted pump radiation) leave the Raman cell simultaneously. We use a ruled grating ($R = 1$ m) to single-out the required anti-Stokes order. Figure 2 shows the arrangement of the main experimental components. A thin MgF_2 flat reflects a small fraction of the VUV beam onto a 0.2 m vacuum monochromator and a solar blind photomultiplier tube (PMT) (Hamamatsu R1259) for reference. The main beam propagates through the plasma to a 1 m VUV monochromator whose exit slit is equipped with the same type of PMT to allow also absorption measurements. Laser-induced-fluorescence radiation is detected perpendicular to the VUV beam. A small volume in the plasma center of length $\sim$1 cm and transverse dimension $\sim$5 mm (determined by the beam diameter) is imaged by a MgF_2 lens ($d = 100$ mm, $R = 75$ mm) onto the photocathode of another gated ($\sim 1\ \mu$s) solar blind PMT. It turned out to be necessary to protect the PMT even in the off mode by a mechanical chopper against the intense background light. The discharge is shut off immediately before the chopper opens the light path to the photocathode. Pulse delay units allow us to trigger the laser pulse and the detection electronics at any time within this time window.

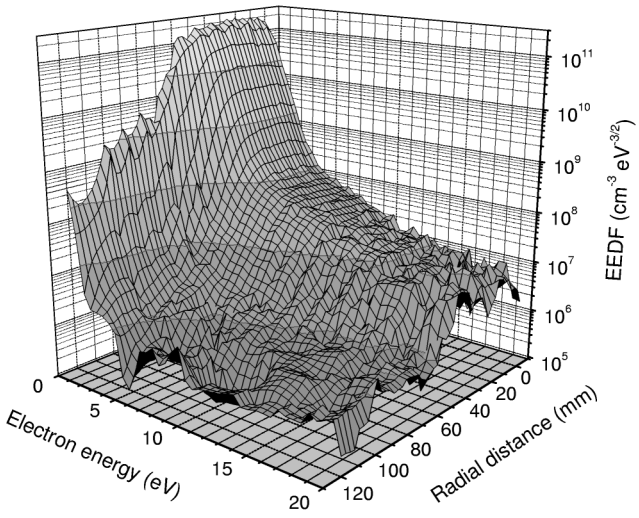

FIG. 1. EEDF as a function of the radial distance from the chamber axis.

Fluorescence lines are recorded by scanning the wavelength (by tuning the dye laser) over the absorption lines in typically 50 spectral steps. 200 signal pulses are summed up at each spectral position whereby the fluorescence light stems from all transitions to lower levels. The signal-to-noise ratio is excellent — even for $B(6, J') \rightarrow X(13, J' + 1)$. The translational temperature, inferred from the width of the Gaussian line profiles, is slightly higher than 300 K. Because of the simultaneous detection of light from transitions to lower levels, it is necessary, in order to arrive at quantitative results, to include in the analysis the transition probabilities, the wavelength dependence of the detection (transmissions, quantum efficiency of the PMT), and the detection geometry (volume, solid angle). The latter calibration is performed by Rayleigh scattering from argon. The quantum efficiency of our PMT was measured by the manufacturer, the spectral data have been taken from the literature [27], and the spectral transmission of the imaging lens was measured in our laboratory.

Figure 3 shows the measured decay times ($1/e$) for $J'' = 1$, $v'' > 4$ states. We are concentrating on high

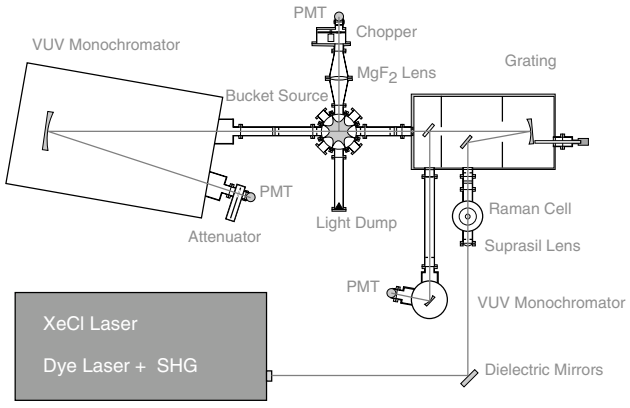

FIG. 2. Experimental arrangement.

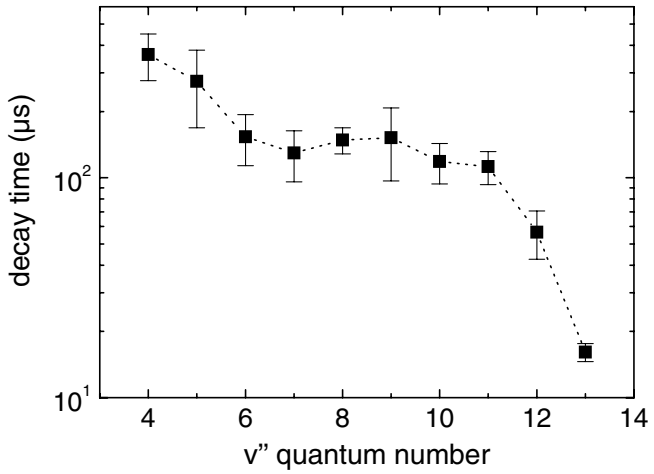

FIG. 3. Measured decay times of the $X(v'', J'' = 1)$ populations.

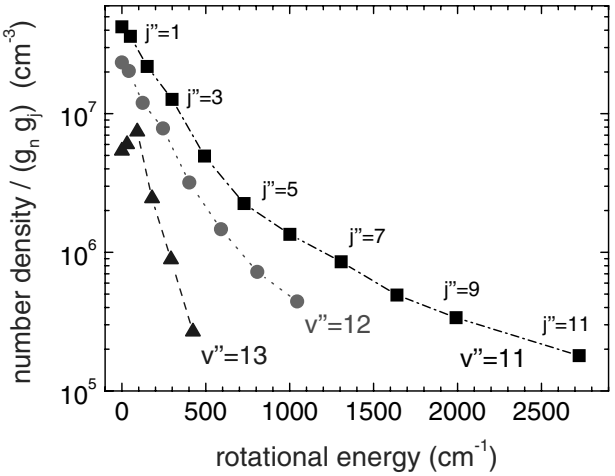

FIG. 4. Measured populations of the rotational substates of v'' states 11–13 as a function of rotational energy, divided by degeneracy factors.

energy states and will not consider states with v'' below 4, where absorption would represent a complication. The vibrational states 6 to 11 exhibit comparable decay times of the order of 100 μs, whereas the highest levels decay much faster. The behavior of the $v'' = 5$, $J'' = 1$ state is irregular in the sense that the population of this state increases during approximately 40 μs before it decays exponentially with the time indicated in the figure. We believe that these decay times can provide, in case of low pressures of the discharge, interesting information on the influence of the wall. The decay time as a function of the rotational excitation was measured for the v'' states 4, 12, and 13. Higher rotational states decay slightly faster (factor 2–4). The dependence of the decay times on the discharge current is only weak. The rotational population turns out, in agreement with earlier results [23–25,28], to be Boltzmann for the first 4 to 5 states, in satisfactory agreement with the translational temperatures inferred from the line profiles, and to exhibit relative overpopulation for higher J''. Figure 4 shows the population densities of the various J'' states for $v'' = 11$, 12, and 13. The results for 11 and 12 are similar to those for lower v'' (temperatures 350 and 300 K, respectively), whereas for $v'' = 13$ a "temperature" of only 150 K results (at a translational temperature from the line profile of 310 K). Figure 5 shows the population distribution as a function of v'' after summation over the rotational states. The suprathermal behavior for high v'' is obvious. Note that the relative shape is in good agreement with calculations by Fukumasa *et al.* [7].

Our measurements of the vibrational and rotational distributions and the EEDF allow us to calculate the production rate $\dot{n}_{H^-}^{\text{prod}}$ of the negative ions in the central section from theoretical cross sections for dissociative attachment according to Eq. (1):

$$\dot{n}_{H^-}^{\text{prod}} = n_e \sum_{v'',J''} n_{H_2}(v'', J'') k_{eH_2}(v'', J'') = n_e 47\ \text{s}^{-1}. \quad (3)$$

It was assumed that the rotational distribution in lower vibrational states is similar to that measured for $v'' = 11$; this is a well-established result which was also seen in other experiments [23–25,28]. We have verified this explicitly for $v'' = 4$. Rotational state dependent cross sections for dissociative attachment can be obtained by scaling the internal energy of the rovibronic states according to the available cross sections—see [16]. Interpolation is necessary for $v'' > 10$. Figure 6 shows the contributions to the production rate. The lower curve neglects the rotational levels, leading to a loss by a factor of 17 in the production rate. The main loss mechanisms for our situation for H^- are fast electron collisional detachment, associative detachment with atomic hydrogen, and mutual neutralization with the positive ions $(H_n^+, n > 1)$. The respective rate coefficients, obtained on the basis of Janev's cross sections [29] are $k_{eH^-} = 1.82 \times 10^{-9}$ cm^3 s^{-1}, $k_{H^+H^-} = 3.1 \times 10^{-8}$ cm^3 s^{-1}, $k_{HH^-} = 8.55 \times 10^{-9}$ cm^3 s^{-1} ($T_{H^-} = T_{H^+} = T_H = 0.05$ eV). The degree of dissociation of 0.5% ($n_H = 1.5 \times 10^{12}$ cm^{-3}) as well as the

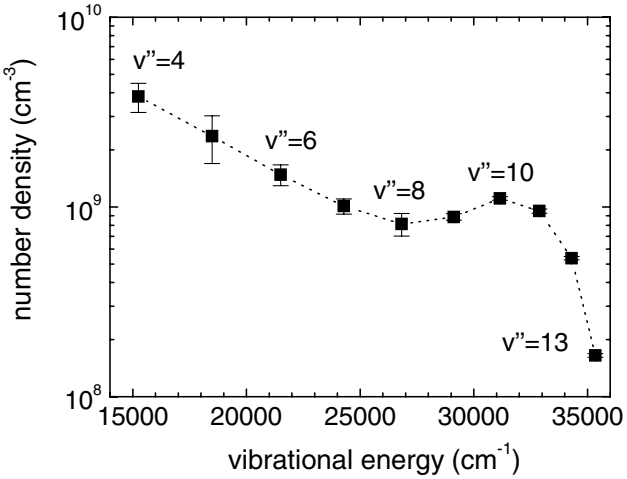

FIG. 5. Vibrational population distribution including rotational levels.

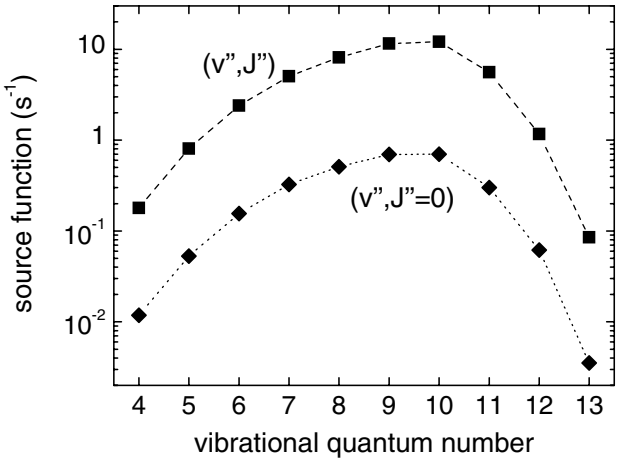

FIG. 6. Vibrational state dependent contributions to the total production rate.

hydrogen temperature T_{H} were determined at a similar source in our group [25]. We assume that the rate coefficient for mutual neutralization with H_2^+ and H_3^+ is similar to that for H^+, hence $\sum n_{H_n^+} = n_e = 1 \times 10^{11}$ cm^{-3}. Radial losses of H^- are neglected because the ions are trapped in the central section. The loss rate $\dot{n}_{H^-}^{\mathrm{loss}}$ is then

$$\dot{n}_{H^-}^{\mathrm{loss}} = n_{H^-}\left(n_e k_{eH^-} + n_H k_{HH^-} + \left(\sum_n n_{H_n^+}\right) k_{H^+H^-}\right)$$
$$= n_{H^-} n_e 4.14 \times 10^{-8}\ \mathrm{cm}^3\,\mathrm{s}^{-1}. \quad (4)$$

Production and loss rates yield the stationary H^- density as $n_{H^-}^{\mathrm{calc}} = 1.14 \times 10^9$ cm^{-3}. We have measured the H^- density using the photodetachment technique [30] in connection with a Langmuir probe. We obtain from this measurement a value of $n_{H^-}^{\mathrm{exp}} = (1.1 \pm 0.3) \times 10^9$ cm^{-3}.

We conclude that our measurements of populations of vibrational and rotational levels and negative ions lead, for our discharge and the selected parameters, to a consistent picture, if we consider dissociative attachment of electrons to rovibrationally excited electronic-ground-state molecules as the dominant mechanism.

We plan to extend our measurements to other experimental parameters and to include deuterium.

We thank Carola Fischer and Jürgen Leistikow for expert technical assistance. This work was funded by the "Deutsche Forschungsgemeinschaft" in the frame of the Sonderforschungsbereich 191, "Grundlagen der Niedertemperaturplasmen."

[1] K. W. Ehlers, J. Vac. Sci. Technol. A **1**, 974 (1983).
[2] A. J. T. Holmes, Plasma Phys. Controlled Fusion **34**, 653 (1992).
[3] J. R. Hiskes, Comments At. Mol. Phys. **19**, 59 (1987).
[4] M. Bacal and D. A. Skinner, Comments At. Mol. Phys. **23**, 283 (1990).
[5] K. N. Leung and K. W. Ehlers, Rev. Sci. Instrum. **55**, 342 (1984).
[6] C. Gorse *et al.,* Chem. Phys. **161**, 211 (1992).
[7] O. Fukumasa, K. Mutou, and H. Naitou, Rev. Sci. Instrum. **63**, 2693 (1992).
[8] D. A. Skinner *et al.,* Phys. Rev. E **48**, 2122 (1993).
[9] P. Berlemont, D. A. Skinner, and M. Bacal, Rev. Sci. Instrum. **64**, 2721 (1993).
[10] O. Fukumasa, J. Phys. D **22**, 1668 (1989).
[11] J. R. Hiskes, Appl. Phys. Lett. **57**, 231 (1990).
[12] M. Bacal, C. Michaut, L. I. Elizarov, and F. El. Balghiti, Rev. Sci. Instrum. **67**, 1138 (1996).
[13] J. R. Hiskes, Appl. Phys. Lett. **69**, 755 (1996).
[14] K. Hassouni, A. Gicquel, and M. Capitelli, Chem. Phys. Lett. **290**, 502 (1998).
[15] J. M. Wadehra and J. N. Bardsley, Phys. Rev. Lett. **41**, 1795 (1978).
[16] J. P. Gauyacq, J. Phys. B **18**, 1859 (1985).
[17] A. P. Hickman, Phys. Rev. A **43**, 3495 (1991).
[18] P. G. Datskos, L. A. Pinnaduwage, and J. F. Kielkopf, Phys. Rev. A **55**, 4131 (1997).
[19] W. G. Graham, Plasma Sources Sci. Technol. **4**, 281 (1995).
[20] J. R. Hiskes, J. Appl. Phys. **70**, 3409 (1991).
[21] M. Péalat, J-P. E. Taran, M. Bacal, and F. Hillion, J. Chem. Phys. **82**, 4943 (1985).
[22] P. J. Eenshuistra, A. W. Kleyn, and H. J. Hopman, Europhys. Lett. **8**, 423 (1989).
[23] G. C. Stutzin *et al.,* Chem. Phys. Lett. **155**, 475 (1989).
[24] G. C. Stutzin *et al.,* Rev. Sci. Instrum. **61**, 619 (1990).
[25] D. Wagner, B. Dikmen, and H. F. Döbele, Plasma Sources Sci. Technol. **7**, 462 (1998).
[26] M. Spaan, A. Goehlich, V. Schulz-von der Gathen, and H. F. Döbele, Appl. Opt. **33**, 3865 (1994).
[27] H. Abgrall *et al.,* Astron. Astrophys. Suppl. Ser. **101**, 273 (1993).
[28] J. H. M. Bonnie, P. J. Eenshuistra, and H. J. Hopman, Phys. Rev. A **37**, 1121 (1988).
[29] R. K. Janev, W. D. Langer, K. Evans, Jr., and D. E. Post, Jr., *Elementary Processes in Hydrogen-Helium Plasmas* (Springer, Berlin, 1987).
[30] M. Bacal, Plasma Sources Sci. Technol. **2**, 190 (1993).